

A Structural Investigation of Anion–Triazole Interactions: Observation of “ π -Pockets” and “ π -Sandwiches”

Nicholas G. White,^[a] Jonathan A. Kitchen,^[a] and Sally Brooker*^[a]

Keywords: Coordination compounds / π interactions / Supramolecular chemistry / Triazoles / N ligands

Eight mononuclear nickel(II) complexes of the ligands 4-amino-3,5-di(2-pyridyl)-1,2,4-triazole (**adpt**) and 4-pyrrolyl-3,5-di(2-pyridyl)-1,2,4-triazole (**pldpt**) with the anions ClO_4^- , BF_4^- , PF_6^- and SbF_6^- have been prepared. In all cases the metal/ligand ratio is 1:3, and the complexes are of the form $[\text{NiL}_3](\text{A})_2 \cdot \text{solvents}$ where L = **adpt** or **pldpt** and A = one of the aforementioned anions. Five of these complexes have been structurally characterized by X-ray crystallography: four of these contain **pldpt** and strong anion– π interactions are observed, with two motifs present in all four structures. One of the anions occupies a “ π -pocket” formed by two coor-

ordinated triazole rings and one coordinated pyridine ring. The other anion only interacts with one triazole ring, which is involved in the pocket around the first anion, such that the triazole ring is “sandwiched” by two anions. Surprisingly, in all four of these complexes, the two triazole centroid–anion distances in the anion–triazole–anion interactions [2.917(7)–3.005(10) Å] are *significantly shorter* than in any of the other types of triazole–anion interactions [3.164(5)–3.456(9) Å].

(© Wiley-VCH Verlag GmbH & Co. KGaA, 69451 Weinheim, Germany, 2009)

Introduction

Since the theoretical description of anion– π (strictly anion– π^*) interactions in 2002^[1] numerous theoretical studies have shown the energetic favourability of contacts between anions and electron-poor aromatic rings.^[2–4] Unambiguous crystallographic evidence of anion– π interactions was provided in 2004,^[5,6] and a number of such interactions have since been observed in the solid state, these interactions often leading to the formation of unusual and interesting supramolecular architectures. Indeed, a recent review of the Cambridge Structural Database (CSD)^[7] shows that there are approximately 3500 structures that contain close contacts between six-membered aromatic rings and anions – the vast majority of which had not been noted by the original authors.^[8]

Dunbar et al. have shown that changing anion size and shape varies the nuclearity of metallacyclophanes, with these structures being templated by anion–tetrazine interactions.^[9] Other authors have used anion– π interactions to generate structures as diverse as molecular baskets,^[5] carousels,^[6] and 3D nets.^[10] Research has also investigated potential applications of these interactions, for example, for anion recognition and binding,^[11] and as synthetic transmembrane anion channels.^[12] Further applications of these

interactions will surely be realized in the near future, as anions play a crucial role in nearly all biological systems.^[13]

Our interest in anion– π systems stems from our research into spin-crossover (SCO) systems. It is well-established that enhancing the cooperativity between metal centres in SCO complexes increases the likelihood of a hysteretic crossover event,^[14,15] a desirable property for technological applications of SCO.^[16] This metal–metal cooperativity may be established through covalent bonds i.e. by synthesising oligonuclear or polymeric systems,^[15,17] or through non-covalent interactions. Previous work has attempted to use hydrogen-bonding^[18] or π – π ^[19] stacking in this manner, but to the best of our knowledge, no work has investigated the use of anion– π interactions to induce cooperativity in SCO systems.^[20]

While much research has looked into pyridazine-, triazine- and tetrazine–anion interactions, we have been unable to find any reports of triazole–anion interactions, or indeed of any five-membered heterocycle–anion interactions. Similarly, given how frequently anion– π interactions occur,^[8] it is surprising that, to the best of our knowledge, no *systematic crystallographic* investigations of this phenomenon have been conducted; i.e., to date no series of closely related structures containing anion– π interactions has been prepared, characterized and analysed. Herein, we present such a study, of a family of mononuclear nickel(II) complexes of the ligands L = **adpt** and **pldpt** with the anions A = BF_4^- , ClO_4^- , PF_6^- , and SbF_6^- [**adpt** = 4-amino-3,5-di(2-pyridyl)-1,2,4-triazole, **pldpt** = 4-pyrrolyl-3,5-di(2-pyridyl)-1,2,4-triazole, Figure 1]. A detailed investigation of the

[a] Department of Chemistry and MacDiarmid Institute for Advanced Materials and Nanotechnology, University of Otago, P. O. Box 56, Dunedin, New Zealand
Fax: +64-3-479-7906

E-mail: sbrooker@chemistry.otago.ac.nz

Supporting information for this article is available on the WWW under <http://www.eurjic.org> or from the author.

interactions between the anions and solvent molecules, and the triazole and pyridine rings, in the resulting $[\text{NiL}_3](\text{A})_2 \cdot \text{solvents}$ complexes is provided.

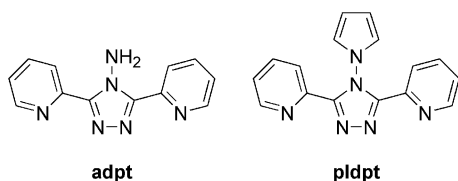


Figure 1. Ligands used in this study.

Results and Discussion

Synthesis

The ligand **adpt** was prepared in two steps following the procedure of Geldard and Lions:^[21] 2-cyanopyridine was condensed with hydrazine hydrate to give 3,6-di(2-pyridyl)-1,2,4,5-dihydro-1H-tetrazine, which rearranged to give the desired ligand when boiled in aqueous hydrochloric acid (Scheme S1). A modification of Mandal's^[22] method was then used to convert **adpt** into **pldpt** (Scheme S1); these authors report using 2,5-dimethoxy-2,5-dihydrofuran in a dioxane/acetic acid mixed solvent system. We have previously used Mandal's procedure to prepare **pldpt**, except that we used 2,5-dimethoxytetrahydrofuran in place of the dihydrofuran.^[23a] While these procedures yield the desired product in high yield, the work-up is reasonably time consuming, as a dark by-product is produced, which must be separated from **pldpt** chromatographically. Furthermore, this method is not particularly robust and reliable—in some instances, we have found that it yields only the dark by-product.

To avoid these problems, we now use ethanol as solvent, and add only a small amount of aqueous HCl to initiate the reaction (the reaction does not proceed if no acid is added) instead of the 50% by volume acetic acid used in Mandal's synthesis.^[22] This prevents the formation of the dark by-product and gives the desired product in slightly higher yield than that previously reported (83%, compared with the 80%^[22] and 77%^[23a] previously achieved). Furthermore, the synthetic work-up is significantly quicker and easier, as simply neutralizing the reaction mixture with triethylamine and reducing it in volume causes analytically pure **pldpt** to crystallize from solution, without the need for chromatography or recrystallization.

The family of eight $[\text{NiL}_3](\text{A})_2 \cdot \text{solvents}$ complexes was readily formed by stoichiometric reactions carried out in CH_3CN , and isolated as pink-purple crystalline solids by vapour diffusion of diethyl ether into the concentrated reaction solution.

Elemental analysis, ESI mass spectrometry fragmentation patterns, and IR spectra of all eight complexes were consistent with proposed structures. Notably, strong peaks at 1088–1089 cm^{-1} $\{[\text{Ni}(\text{adpt})_3](\text{ClO}_4)_2, (\mathbf{1ClO}_4)\}$ and $[\text{Ni}(\text{pldpt})_3](\text{ClO}_4)_2, (\mathbf{2ClO}_4)\}$, 1057 cm^{-1} $\{[\text{Ni}(\text{adpt})_3](\text{BF}_4)_2,$

$(\mathbf{1BF}_4)$ and $[\text{Ni}(\text{pldpt})_3](\text{BF}_4)_2, (\mathbf{2BF}_4)\}$, 843 cm^{-1} $\{[\text{Ni}(\text{adpt})_3](\text{PF}_6)_2, (\mathbf{1PF}_6)$ and $[\text{Ni}(\text{pldpt})_3](\text{PF}_6)_2, (\mathbf{2PF}_6)\}$ and 660–661 cm^{-1} $\{[\text{Ni}(\text{adpt})_3](\text{SbF}_6)_2, (\mathbf{1SbF}_6)$ and $[\text{Ni}(\text{pldpt})_3](\text{SbF}_6)_2, (\mathbf{2SbF}_6)\}$ were observed, consistent with the respective non-coordinated anion.

UV/Vis Spectroscopy

Goodwin and colleagues had some success in rationalizing the magnetic behaviour of $[\text{Fe}^{\text{II}}\text{L}'_3]\text{A}_2$ complexes, where L' is a 3-(2-pyridyl) five-membered heterocycle ligand, on the basis of the UV/Vis spectra of the analogous nickel(II) complexes.^[24,25] Given that we have established a general synthetic route to 4-substituted 3,5-di(2-pyridyl)-1,2,4-triazole **Rdpt** ligands,^[26] we attempted to distinguish between the ligand fields imposed by these ligands using UV/Vis spectroscopy. Hence, we recorded both the solution and solid-state UV/Vis spectra of the nickel(II) complexes **1BF₄** and **2BF₄**—the ligands **adpt** and **pldpt** having triazole N₄-substituents that differ markedly in their electron-donating/-withdrawing properties (to give a general feel for this difference the Hammett constants are: NH_2 , *para*: −0.66, *ortho*: −0.16; pyrrolyl, $\sigma_1 = 0.17$ ^[27])—in the expectation that this would inform the subsequent iron(II) chemistry of these ligands.

Unfortunately, as shown in Figure S1, the UV/Vis peaks were too broad to distinguish between the small differences in $10Dq$ caused by this remote ligand modification. Both complexes show ${}^3\text{A}_{2g} \rightarrow {}^3\text{T}_{1g}$ transitions at approximately 19,000 cm^{-1} and ${}^3\text{A}_{2g} \rightarrow {}^3\text{T}_{2g}$ transitions at 11,600 cm^{-1} .

X-ray Crystallography

Single crystals of all four **pldpt** complexes, **2ClO₄**· $\text{CH}_3\text{CN} \cdot 0.7(\text{C}_2\text{H}_5)_2\text{O} \cdot 0.3\text{H}_2\text{O}$, **2BF₄**· $\text{CH}_3\text{CN} \cdot 0.5(\text{C}_2\text{H}_5)_2\text{O}$, **2PF₆**· $\text{CH}_3\text{CN} \cdot (\text{C}_2\text{H}_5)_2\text{O}$ and **2SbF₆**· $\text{CH}_3\text{CN} \cdot (\text{C}_2\text{H}_5)_2\text{O}$, and of one **adpt** complex, **1SbF₆**· $1.5\text{CH}_3\text{CN} \cdot 0.58(\text{C}_2\text{H}_5)_2\text{O}$, were grown by the vapour diffusion of diethyl ether into the acetonitrile reaction solution. All complexes contain a central nickel(II) ion binding three ligands through just one of the two potential bidentate binding pockets per ligand (Figures 2, 3, 4, and 5; Tables S1–S3 in the Supporting Information). The coordination of these bidentate pockets, each comprising a pyridine nitrogen and an N₁ of a triazole ring, gives the nickel(II) ions N₆ distorted octahedral geometries (Table S2), with all complexes adopting the *meridional* configuration. No crystallographically-imposed symmetry is present within any of the cations. Two crystallographically independent non-coordinated counterions per nickel(II) are also present in each structure (Figures 2, 3, 4, 5; S2–S6), along with some solvent molecules. Some structures contained disorder and this is detailed in the Supporting Information.

The sole structure containing **adpt** contains two Ni-(**adpt**)₃²⁺ cations and four SbF₆ counter anions, as well as some solvent molecules, in the asymmetric unit, and crystallizes in the triclinic space group $P\bar{1}$.

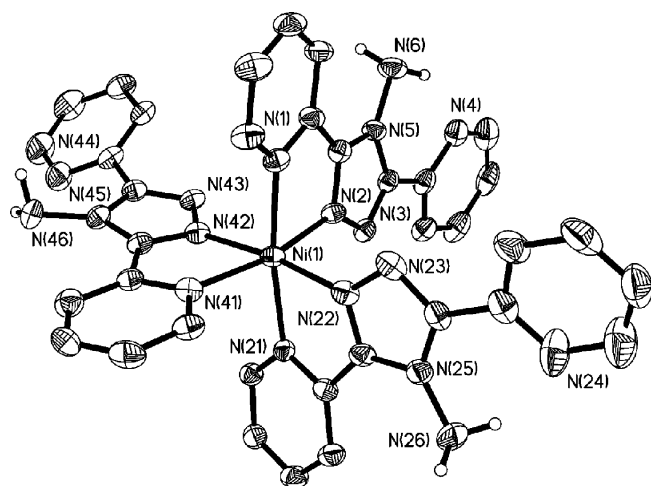


Figure 2. Perspective view of one of the two crystallographically independent cations of $1\text{SbF}_6 \cdot 1.5\text{CH}_3\text{CN} \cdot 0.58(\text{C}_2\text{H}_5)_2\text{O}$ (hydrogen atoms omitted for clarity). See Figures S5 and S6 for the structure of the other cation, and an OFIT diagram of the two cations.

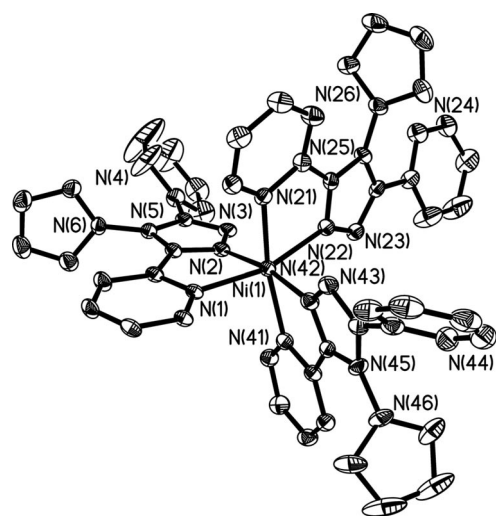


Figure 3. Perspective view of $2\text{BF}_4 \cdot \text{CH}_3\text{CN} \cdot (\text{C}_2\text{H}_5)_2\text{O}$ (solvent molecules, hydrogen atoms and non-coordinated pyridine ring twirl disorder omitted for clarity). The structures of the cations of $2\text{ClO}_4 \cdot \text{CH}_3\text{CN} \cdot 0.7(\text{C}_2\text{H}_5)_2\text{O} \cdot 0.3\text{H}_2\text{O}$, $2\text{PF}_6 \cdot \text{CH}_3\text{CN} \cdot (\text{C}_2\text{H}_5)_2\text{O}$ and $2\text{SbF}_6 \cdot \text{CH}_3\text{CN} \cdot (\text{C}_2\text{H}_5)_2\text{O}$ (Figures S2–S4) are very similar.

The four structures containing **pldpt** all crystallize in the monoclinic space group $P2_1/n$ and have just one $\text{Ni}(\text{pldpt})_3^{2+}$ cation and two counter anions, along with solvent molecules, in the asymmetric unit. These **pldpt**-containing complexes are structurally very similar to one another in the solid state. The unit-cell dimensions show only a slight increase in unit-cell size and axis lengths with increasing anion size (Tables 1, and S1 in the Supporting Information). In all four **pldpt** complexes there is one acetonitrile solvate and one further region of solvent (although the exact nature and occupancy of the latter site varies between structures) per cation.

Table 1. Comparison of axis cell lengths, unit-cell volume and anion volume for the structures, $2\text{BF}_4 \cdot \text{CH}_3\text{CN} \cdot 0.5(\text{C}_2\text{H}_5)_2\text{O}$, $2\text{ClO}_4 \cdot \text{CH}_3\text{CN} \cdot 0.7(\text{C}_2\text{H}_5)_2\text{O} \cdot 0.3\text{H}_2\text{O}$, $2\text{PF}_6 \cdot \text{CH}_3\text{CN} \cdot (\text{C}_2\text{H}_5)_2\text{O}$ and $2\text{SbF}_6 \cdot \text{CH}_3\text{CN} \cdot (\text{C}_2\text{H}_5)_2\text{O}$.

	2BF_4	2ClO_4	2PF_6	2SbF_6
a [Å]	16.9235(16)	16.9779(17)	17.4949(11)	17.729(3)
b [Å]	23.175(2)	23.178(2)	23.3993(14)	23.708(3)
c [Å]	15.3132(15)	15.4992(16)	15.8469(9)	16.175(3)
V [Å ³]	5534.0(9)	5589.2(9)	5886.7(6)	6131.3(16)
Anion volume [Å ³] ^[28]	38	47	54	63

As expected, the nickel–nitrogen bond lengths and angles vary little between the five structures (Table S2). Notably the nickel–triazole (trz) bond lengths are significantly shorter than nickel–pyridine (py) bonds in all cases [Ni–trz 2.035(5)–2.078(3) Å, Ni–py 2.100(5)–2.149(5) Å, Table S2]. Unsurprisingly, *cis*-N–Ni–N bond angles are close to 90° [largest deviation: 12.70(19)°, mean deviation: 6.6°, Table S2] and *trans*-N–Ni–N bond angles are close to 180° [largest deviation: 18.1(3)°, mean deviation: 12.5°, Table S2], so that the nickel ions show only a small distortion from an ideal octahedral geometry.

The situation regarding twisting of the individual ligands away from planarity is more complicated. In the sole **adpt**-containing structure (Figure 2, S5 and S6) there are small twists, of 1–13°, between the coordinated pyridine ring and triazole ring (Table S3). A somewhat larger twist, of 11–32°, is seen between the triazole and non-coordinated pyridine ring, but the extent of the twist remains modest as each of the six non-coordinated pyridine ring nitrogen atoms hydrogen-bonds to a proton on the amino nitrogen of the same **adpt** ligand.

The four **pldpt**-containing complexes (Figures 3, 4, and 5, S2–4) all show two different types of ligand twist: each cation contains two ligand strands that have a very small twist between the coordinated pyridine and triazole rings (< 7°), with a much larger twist seen between the non-coordinated pyridine and triazole rings [38.9(5)–50.78(16)°, Table S3]. However, the third ligand strand behaves differently: twists of ca. 14–15° are observed between both the coordinated pyridine and triazole rings, and between the non-coordinated pyridine and triazole rings. That is, there is no significant difference between the triazole–pyridine mean plane intersects for the coordinated vs. non-coordinated pyridine rings. Both of the twists are in the same direction, so that the two pyridine rings are at angles of ca. 28–30° to one another. In all four complexes, this ligand strand is the only one that contains a coordinated pyridine–anion interaction (see later), so presumably the larger than expected coordinated pyridine–triazole twist facilitates a more favourable geometry for this interaction. The non-coordinated pyridine on this ligand strand is reasonably close to a coordinated pyridine on one side and a region of solvent (partial or full occupancy diethyl ether/water depending on the structure): it appears that this small triazole–non-coordinated pyridine twist arises to prevent unfavourable steric repulsions with these groups. In all four **pldpt** complexes there is a large twist, 80.4(4)–85.3(4)°

(Table S3), around the triazole–pyrrole N–N bond, similar to previously observed mean plane intersects for complexes of **pldpt** [82.4(3)–88.8(1)]^[22,23a] and for the free ligand in the solid state [81.9(1) and 82.4(1)].^[23a]

The only structure to contain significant hydrogen-bonding was also the only structurally characterized complex of **adpt**, **aSbF₆**·1.5CH₃CN·0.58(C₂H₅)₂O. It contains hydrogen bonds from all twelve amino protons, to SbF₆ fluorine atoms, non-coordinated **adpt** pyridine nitrogen atoms, a diethyl ether oxygen atom and an acetonitrile nitrogen atom [N–H···A 2.827(8)–3.483(9) Å, angle N–H···A 123.6–170.3°, Table S9]. Interestingly, this structure contained very little in the way of anion–π interactions, in contrast to all other structures, of **pldpt**, which showed numerous and strong anion–π contacts (see later).

Anion–π Interactions

The two complexes present in the asymmetric unit of the sole **adpt** complex only make two anion–π contacts that are shorter than 3.5 Å. Both are quite long [F···centroid 3.304(7) and 3.492(9) Å], and may well be due to crystal packing forces rather than genuine anion–π interactions (so these are not considered further in the anion–π discussion below). This result quite surprising as other structures containing the ligand **adpt** have shown moderate anion–π inter-

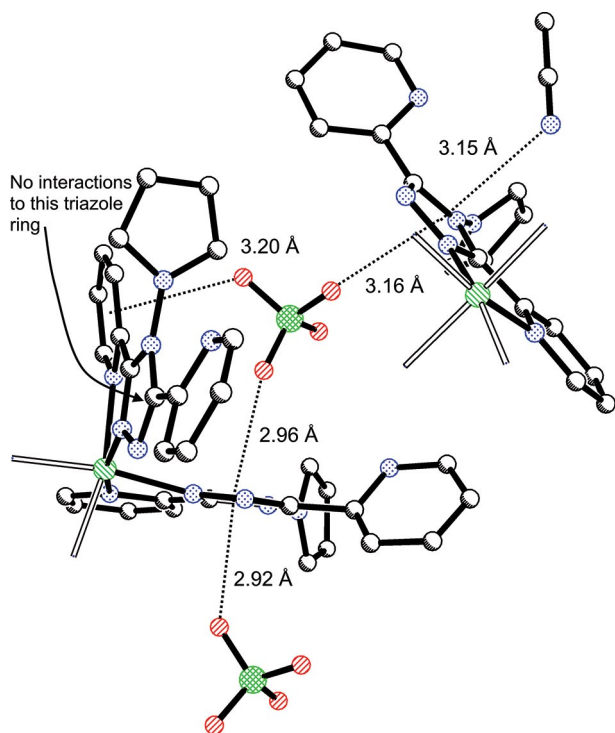


Figure 4. Diagram showing anion–π and CH₃CN–π interactions present in **2ClO₄**·CH₃CN·0.7(C₂H₅)₂O·0.3H₂O. These include both π-pocket and π-sandwich interactions; the interactions observed in **2BF₄**·CH₃CN·(C₂H₅)₂O (Figure S7) are very similar. Of the three crystallographically unique triazole rings, the one indicated by an arrow is not involved in any anion/solvent···π interactions. All numbers indicate X···centroid distances. Hollow bonds indicate ligand strands that have been removed for clarity.

actions with ClO₄ anions [trz centroid···X 3.044 Å,^[29] trz centroid···X 3.138 Å,^[30] and we have recently observed extremely strong [trz centroid···X 2.790(5) Å] interactions in the iron(II) analogue of **1BF₄**, i.e. [Fe^{II}(**adpt**)₃](BF₄)₂·0.5(C₂H₅)₂O.^[31]

In all four structures containing **pldpt**, one of the two anions in the asymmetric unit interacts with only one aromatic ring (Figures 4 and 5, Figures S7 and S8). In all cases, this is a triazole ring, and the interaction is strong [trz centroid···X 2.917(7)–3.005(10) Å, X = O for **2ClO₄**, X = F for **2BF₄**, **2PF₆** and **2SbF₆**]. This does not include the minor position of the disordered PF₆ in **2PF₆**. For full details of all anion–π interactions (see Tables S4–S8). The other anion sits in a “π-pocket” provided by two triazole rings and one coordinated pyridine ring. One of these triazole rings is the same one that interacts with the other anion, so it is “sandwiched” by these two anions. This second anion–π interaction is also strong [trz centroid···X 2.956(7)–3.005(4) Å], despite the fact that overall *this is an anion–π–anion interaction*. The interactions with the other triazole and the pyridine of the π-pocket are weaker and vary slightly for the tetrahedral anions compared to the octahedral anions. The tetrahedral anions show moderate anion–π interactions with both the pyridine and triazole rings [py centroid···X 3.202(7), 3.265(5) Å; trz centroid···X 3.164(5), 3.224(4) Å, for **2ClO₄** and **2BF₄**, respectively]. The octahedral anions show a moderate interaction with a pyridine ring, coupled with a much weaker interaction to this same pyridine from

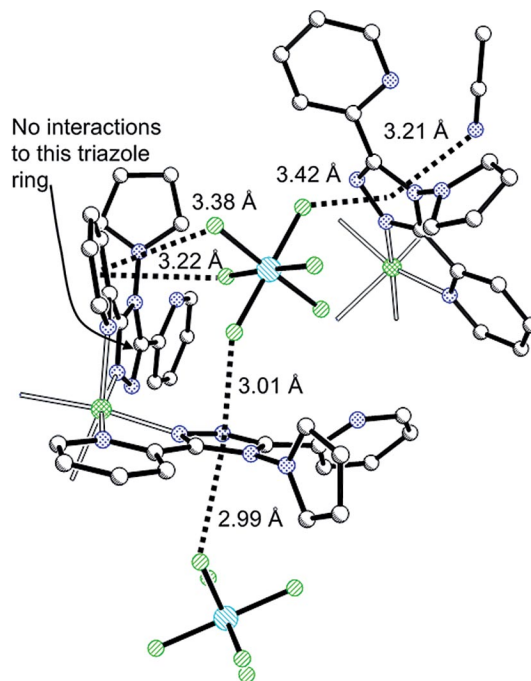


Figure 5. Diagram showing anion–π and CH₃CN–π interactions present in **2SbF₆**·CH₃CN·(C₂H₅)₂O. Of the three crystallographically unique triazole rings, the one indicated by an arrow is not involved in any anion/solvent···π interactions. All numbers indicate X···centroid distances. Hollow bonds indicate ligand strands that have been removed for clarity. The arrangement in **2PF₆**·CH₃CN·(C₂H₅)₂O is very similar (Figure S8).

a different fluorine on the same anion, as well as weak interactions between the anion and the other triazole of the π -pocket [**2PF₆**; py centroid...F 3.185(4), 3.433(4) Å; trz centroid...F 3.454(13) Å, **2SbF₆**; py centroid...F 3.218(10), 3.376(9) Å; trz centroid...F 3.420(10) Å].

The extent of centering of the anion above the centre of the involved aromatic ring is described by the acute angle of the ring mean plane–ring centroid–X, with an angle of 90° implying the anion atom is directly above the ring centroid and smaller angles showing correspondingly poorer centering. In these structures the strong interactions, where two anions sandwich one triazole ring, have angles ranging from 70.9 to 83.5°, with the angles for the other, weaker interactions ranging from 55.1 to 79.3°. The angle of the central atom of the anion–X–ring centroid reveals how directly X is “pointing” at the ring: these angles range between 128.4(3) and 151.7(3) for the strong “sandwiching” interactions, and 100.9(3) and 171.0(3) for the other, weaker interactions.

For these complexes, shorter anion– π contacts are correlated ($P = 0.001$) with mean plane–centroid–X angles that are closer to 90° (Figure 6). While this is the intuitively expected result: a close (and hence strong^[32]) anion– π interaction would be expected to involve an anion positioned close to the “ideal” location directly above the ring centroid, it disagrees with the general trend found by Reedijk et al.^[8] in their survey of the CSD.^[7] In that survey it seems that the size of the mean plane–centroid–X angle has very little effect on the X...centroid distance, if anything shorter distances being weakly associated with smaller (further from 90°) angles.

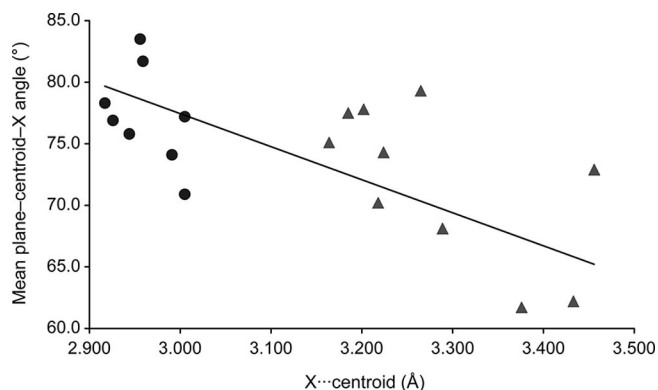


Figure 6. Scatter plot and trend line ($R^2 = 0.48$, $P = 0.001$) showing relationship between mean plane–centroid–X angle and X...centroid distance for complexes containing pldpt ligand. The anion-sandwiching interactions are shown as blue circles, and other anion– π interactions are shown as red triangles.

A correlation ($P = 0.036$) is seen between the central atom–X...centroid angle and X...centroid distance (Figure S9). However, this analysis is complicated as the anions in the π -pocket have more than one oxygen or fluorine atom interacting with aromatic rings and so must compromise and arrange themselves in such a way that all of these atoms are in appropriate locations with respect to the aromatic

rings. Interestingly, the four anions that interact with only one triazole ring (one anion in each of the four pldpt-containing structures), and as such have more freedom to attain the most favourable orientation to interact with the triazole ring, have anion central atom–X...centroid angles of 128.4(3) to 134.8(3)°.

As expected based on the far greater π -acidity^[3] of a triazole ring compared with a pyridine ring, anion– π interactions involving the triazole rings are generally shorter than those involving the pyridine rings (Figure S10). The mean plane–centroid–X angles are also generally closer to 90° for the triazole–anion interactions. Only *coordinated* pyridine rings are involved in the observed anion– π interactions; this is expected, as coordination of a formally positively charged metal ion withdraws electron density from the ring, increasing its π -acidity, and favouring an interaction with an electron-rich moiety such as an anion.

Anion– π interactions involving the tetrahedral anions BF₄ and ClO₄ vary slightly from those involving the octahedral anions PF₆ and SbF₆. While the anion-sandwiching interactions are reasonably similar (see next paragraph), those involved in the π -pocket are somewhat different (Figure S11). Notably, interactions to the non-sandwiched triazole are much weaker for the octahedral anions. This is presumably because the octahedral anions feature two interactions with a coordinated pyridine ring (one interaction comparable with those found in the structures containing tetrahedral anion, and one weaker interaction), and so optimising the geometries for these interactions comes at a cost to the triazole–anion interaction.

The anion sandwiching X...centroid distances increase slightly ClO₄ \approx BF₄ < PF₆ < SbF₆ (mean X...centroid values: X_{BF₄/ClO₄} = 2.956 Å; X_{PF₆} = 2.975 Å; X_{SbF₆} = 2.998 Å). The tetrahedral anions presumably show slightly shorter interactions as the single negative charge is spread over four atoms rather than six, making each F/O more δ^- in the tetrahedral anions, than in the octahedral. However, not too much should be read into any of these differences as they are very small (≈ 0.04 Å), and only a small number of data points are being analysed.

The formation of a π -pocket around one anion in each of the four structures containing pldpt offers an ideal opportunity to study anion– π interactions in detail. The anion is the only moiety present in this pocket, and so should be able to orient itself purely to optimize anion– π interactions. This optimized orientation seems to involve close contacts with two triazole rings and one pyridine ring, as this is observed in all four complexes, whether a tetrahedral or octahedral anion is used. It is surprising, therefore, that *by far the shortest anion– π contact is with the triazole ring that is already forming a short anion– π contact with the other anion.* Based on the simple electrostatic description of anion– π interactions to date,^[2] this should not occur. Rather, this description predicts that one anion– π interaction should remove much of the aromatic ring's π -acidity, hence reducing its propensity for further anion– π interactions, i.e. in the systems described here, this would lead to an (incorrect) expectation that either the anion in the π -pocket would

move away from the triazole that is already interacting with an anion to form short interactions with the other “free” triazole ring present in the pocket, or the anion that is not located in the π -pocket would interact with the third triazole that is not involved with the π -pocket (and which should therefore be more π -acidic). Such a finding was observed by Reedijk et al.^[3] where a nitrate-triazine-nitrate arrangement contained one moderate (O \cdots triazine 3.201 Å) and one weak (O \cdots triazine 3.502 Å) interaction. The authors commented that “the longer distance observed, when two anions are interacting with the triazine, can be rationally explained as follows: the binding of the first nitrate gives the electron density to the electron-poor ring; as a result, this ring becomes less electron-deficient and the interaction is weaker for the second anion.”^[3] However, this is clearly not the case in our system.

As well as this strong sandwiching interaction, there is also a weaker sandwiching of a triazole ring, as the triazole ring that weakly interacts with the anion is also involved in another interaction—forming a close contact with the CH₃CN solvate (see next section).

To summarize, there are three triazole rings in each complex: one is involved in two strong contacts to electron-rich moieties [2.917(7)–3.005(4) Å], one is involved in two weaker contacts [3.090(9)–3.454(13) Å], and one is not involved in any interactions (closest contact > 3.6 Å). *This arrangement occurs even when the size and shape of the anion is varied substantially.* While we cannot definitively discount crystal packing forces as the cause of these interactions, there seems no reason for these to be a factor in our system, as the anion in the π -pocket is essentially isolated. Instead, we suggest that there may be an electronic factor that favours this anion– π -anion sandwiching arrangement. This cannot be accounted for by the above simple electrostatic model of anion– π interactions—it appears that more complex factors are also involved, possibly leading to synergic anion– π binding of anions. We hope that this publication will help to stimulate further theoretical studies by appropriate experts in the field as it would be valuable to improve our understanding of the nature of these more complex interactions.

There are many examples in the literature of structures that show strong anion– π -anion sandwiching interactions. For example, a number of metal complexes of 3,6-di(2-pyridyl)-1,2,4,5-tetrazine (**dpztz**) or 3,6-di(2-pyrazinyl)-1,2,4,5-tetrazine (**dpztz**) have been prepared by the groups of Dunbar^[9,32,33] and Champness^[34] that contain an anion–tetrazine–anion arrangement with centroid–anion distances as short as 2.75 Å for both anions. It is worth noting, however, that in most structures there is an “excess” of anion, when compared with π -deficient aromatic rings, particularly given that one anion may be involved in interactions with a number of π -rings. Hence, in the **dpztz** and **dzpztz** complexes, there are no tetrazine rings that are not involved in anion– π interactions. Similarly, the **pldpt** ligand has previously shown anion– π -anion sandwiching interactions (F \cdots centroid 2.89–3.07 Å) in the complexes [M₂(**pldpt**)₂(CH₃CN)_m(H₂O)_n](BF₄)₄ (M = Fe²⁺,^[23b] Co²⁺, Zn²⁺, m =

2, n = 2; M = Ni²⁺, m = 4, n = 0).^[23a] However, this is enforced by the stoichiometry of the system as there are four anions and only two triazole rings in each dinuclear complex, and so if each anion is to interact with a π -ring, a sandwiching arrangement must occur.

What is unusual about the complexes reported herein is that we see an *anion– π -anion sandwiching arrangement, despite the presence of triazole rings that are not involved in anion– π interactions.* In a search of the CSD,^[7] no anion– π -anion sandwiching interactions (X \cdots centroid < 3.1 Å) were found for triazine, tetrazine or triazole rings with halogen or oxygen containing anions that also had a “spare” (i.e. not involved in anion– π interactions) ring in the structure.

CH₃CN– π Interactions

The structure containing **adpt** does not contain any significant CH₃CN– π interactions (N \cdots centroid > 3.4 Å). All four structures containing **pldpt** show short contacts between the nitrogen of an acetonitrile solvate and a triazole ring. These N \cdots centroid distances range from 3.090(9) Å in **2BF₄** to 3.212(14) Å in **2SbF₆**. In all cases, the ring plane–ring centroid–acetonitrile nitrogen is very close to 90° (85.0–87.3°). Interestingly, all of these angles are much closer to 90° than any of the anion– π interactions (ring plane–ring centroid–anion atom: 55.1–83.5°).

Heterocycle–CH₃CN interactions have previously been calculated to be energetically favourable, and observed crystallographically (albeit with a disordered CH₃CN molecule) by Reedijk et al. for complexes involving a 1,3,5-triazine moiety.^[35] These authors calculated that the optimum geometry for an acetonitrile molecule and a free 1,3,5-triazine ring had a centroid–CH₃CN nitrogen distance of 3.116 Å, with a mean plane–centroid–N angle of 90°, and the acetonitrile being approximately planar with the triazine ring (i.e. a C \equiv N \cdots centroid angle of approximately 90°). Crystallographically, they observed the disordered CH₃CN to have two sites (each at 50% occupancy), with the two centroid–N distances being 3.087(5) and 3.249(5) Å and the mean plane–centroid–N angles being 75.48(3) and 82.84(3)°, respectively. It is interesting to note that while the mean plane–centroid–N angles we report are very close to the 90° calculated as ideal for a 1,3,5-triazine–acetonitrile interaction (indeed, much closer than those observed by Reedijk et al.),^[35] the C \equiv N \cdots centroid angles range from 112.5(11) to 119.7(7)°, quite far from 90°. Presumably, this is due to steric repulsion enforced by other parts of the ligand and complex, that would not be involved in Reedijk et al.’s calculation, which involved only the free 1,3,5-triazine ring. We are aware of only one further report of a crystallographically observed CH₃CN– π interaction,^[36] although that interaction was reasonably weak [centroid \cdots N 3.348(11) Å, mean plane–centroid \cdots N angle 80.16(2)°].

Unlike the anion– π interactions, no significant correlation was observed between N \cdots centroid distance and mean plane \cdots centroid \cdots N angles, although any possible

trend may be hidden by the very small sample size (there are only four CH₃CN interactions across the four complexes). Despite the small amount of data, a significant correlation ($P = 0.036$) is seen between shorter N \cdots centroid distances and increasing \langle C–N \cdots centroid angles (Figure S12). This is despite this increase in angle moving the CH₃CN further from the planar (i.e. C \equiv N–centroid angle of $\approx 90^\circ$) arrangement calculated to be favourable by Reedijk et al.^[35]

It is worth noting that while the occupancy and nature of the second solvent region [0.5 occupancy (C₂H₅)₂O, full occupancy (C₂H₅)₂O or 0.7(C₂H₅)₂O/0.3H₂O] in each of the four structures varies, there is one full occupancy CH₃CN in each structure, suggesting that this interaction is favourable enough to prevent disorder of this solvent within the lattice.

Conclusions

A series of eight mononuclear nickel(II) complexes has been prepared. Four complexes containing the ligand **pldpt** and one containing **adpt** have been structurally characterized in the solid state by X-ray crystallography. The complex of **adpt** contains only very weak anion– π interactions; the four complexes of **pldpt** contain both strong anion– π interactions and CH₃CN– π interactions. In all four complexes, two types of anion– π interactions are observed: one anion interacts with only one triazole ring, while the other anion is situated in a π -pocket provided by two triazole rings and one pyridine ring. The anion is the only moiety in this pocket, and so should be free to adopt the most energetically favourable conformation for anion– π bonding: surprisingly, the anion forms its shortest interaction with the triazole ring that is already interacting with an anion. The other triazole ring involved in the π -pocket around an anion also interacts with a nitrogen donor from an acetonitrile solvate so that this triazole is also sandwiched by electron-rich moieties. Conversely, the third triazole ring does not interact with any anions or acetonitrile molecules. While we cannot definitively discount crystal packing forces as the cause of the observed sandwiching interactions, we cannot see why this should be the case in this particular system, particularly given that this arrangement occurs for all four complexes—even when the size and shape of the anion is varied substantially. Instead, we suggest that the present model of anion– π interactions as a simple electrostatic attraction between an electron-rich moiety and an electron-poor π -ring may need to be modified to allow for more complex electronic effects.

Experimental Section

General Remarks: IR spectra were recorded as pressed KBr discs with a Perkin–Elmer Spectrum BX FT-IR spectrophotometer between 400 and 4000 cm^{–1}. UV/Vis/NIR spectra were recorded with a Varian CARY 500 Scan UV/Vis/NIR spectrophotometer between 200 and 2000 nm. ESI mass spectra were recorded at the University

of Otago on a Bruker MicrOTOF_Q spectrometer in acetonitrile. ¹H NMR spectra were recorded with a Varian INOVA-500 spectrometer at 25 °C.

Single-crystal X-ray diffraction data for all complexes were collected with a Bruker Kappa Apex II area detector diffractometer (University of Otago) at 83 K. In all cases graphite-monochromated Mo- K_α radiation ($\lambda = 0.71073 \text{ \AA}$) was used. All data sets were corrected for absorption using SCALE.^[37] The structures were solved using SHELXS-97.^[38] All structures were refined against F^2 using all data by full-matrix least-squares techniques with SHELXL-97.^[38] All non-hydrogen atoms were modelled anisotropically except for some disordered/partial occupancy solvents or non-coordinated pyridine rings (see Supporting Information for full details). Hydrogen atoms were inserted at calculated positions, except for the amino protons in **1SbF₆·1.5CH₃CN·0.58(C₂H₅)₂O**, and rode on the atoms to which they are attached (including isotropic thermal parameters which were equal to 1.2 times the attached non-hydrogen atom). The amino protons in **1SbF₆·1.5CH₃CN·0.58(C₂H₅)₂O** were found in the difference map and their coordinates fixed. Crystal structure determination details are summarized in Table S1.

CCDC-696906 [for **2ClO₄·CH₃CN·0.7(C₂H₅)₂O·0.3H₂O**], -696907 [for **2BF₄·CH₃CN·0.5(C₂H₅)₂O**], -696908 [for **2PF₆·CH₃CN·(C₂H₅)₂O**], -696909 [for **2SbF₆·CH₃CN·(C₂H₅)₂O**], -696910 [for **1SbF₆·1.5CH₃CN·0.58(C₂H₅)₂O**], contain the supplementary crystallographic data for this paper. These data can be obtained free of charge from The Cambridge Crystallographic Data Centre via www.ccdc.cam.ac.uk/data_request/cif.

Ligand **adpt** was prepared as described previously.^[21] Acetonitrile (MeCN) was HPLC-grade, and distilled from over calcium hydride before use; triethylamine was also distilled from calcium hydride prior to use. All other starting materials or solvents were bought commercially and used as received.

Caution: While no problems were encountered in the course of this work, reactions involving N₂H₄·H₂O may form potentially explosive mixtures so must be carried out with extreme caution. Similarly, ClO₄[–] salts are potentially explosive so should be handled with appropriate care.

4-Pyrrolyl-3,5-di(2-pyridyl)-1,2,4-triazole (pldpt): Ligand **adpt** (0.477 g, 2.00 mmol) was refluxed in ethanol (30 mL) containing concentrated aqueous hydrochloric acid ($\approx 37\%$, 0.3 mL) and 2,5-dimethoxytetrahydrofuran (0.31 mL, 0.32 g, 2.4 mmol) for two hours, during which time all material dissolved to give a pink solution. This was cooled to room temperature and triethylamine (1 mL) added, causing the pink solution to turn yellow. Reducing this solution in volume to 8 mL under reduced pressure caused a white, crystalline solid to precipitate. This was isolated by filtration, thoroughly washed with distilled water (25 mL) and dried in vacuo. Yield 0.481 g (83%). C₁₆H₁₂N₆ (288.31): calcd. C 66.65, H 4.20, N 29.15; found C 66.42, H 4.25, N 29.44. ¹H NMR spectroscopic data were consistent with those previously reported.^[22,23a]

General Procedure for Synthesis of Complexes 1ClO₄, 1BF₄, 2ClO₄ and 2BF₄: One equivalent of [Ni(H₂O)₆]X₂ (X = ClO₄[–] or BF₄[–]) was stirred with three equivalents of the appropriate ligand in MeCN at room temperature. After a few minutes, all material dissolved to give a pale pink solution. This was subjected to diethyl ether vapour diffusion, yielding pale pink-purple microcrystals, which were isolated by filtration, washed with diethyl ether, and dried thoroughly in vacuo. Yields ranged from 59% to 73%.

[Ni(adpt)₃](ClO₄)₂·3H₂O (1ClO₄·3H₂O): The reaction of [Ni(H₂O)₆](ClO₄)₂ (37 mg, 0.10 mmol) and **adpt** (71 mg, 0.30 mmol) in

6 mL of MeCN according to the procedure described above gave pale pink-purple microcrystals. Yield 61 mg (59%). IR (KBr): $\tilde{\nu}$ = (inter alia) 3279 (m), 3112 (m), 3079 (m), 3021 (m), 1633 (m), 1607 (m), 1591 (m), 1573 (w), 1495 (m), 1456 (s), 1428 (s), 1294 (w), 1259 (m), 1088 (br. vs), 1016 (m), 793 (m), 749 (m), 700 (m), 624 (m), 608 (w) cm^{-1} . ESI-MS (pos.): m/z = 1085 $[\text{Na}\cdot\text{Ni}(\text{adpt})_3(\text{PF}_6)_2]^+$, 647 $[\text{Na}_3(\text{adpt})(\text{PF}_6)_2]^+$, 267. $[\text{Ni}(\text{adpt})_3]^{2+}\cdot\text{1ClO}_4\cdot\text{3H}_2\text{O}$. $\text{C}_{36}\text{H}_{36}\text{Cl}_2\text{N}_{18}\text{NiO}_{11}$ (1026.38): calcd. C 42.13, H 3.54, N 24.56; found C 41.94, H 3.32, N 24.40.

[Ni(adpt)₃(BF₄)₂(1BF₄): The reaction of $[\text{Ni}(\text{H}_2\text{O})_6](\text{BF}_4)_2$ (34 mg, 0.10 mmol) and **adpt** (71 mg, 0.30 mmol) in 12 mL of MeCN according to the procedure described above gave pale pink-purple microcrystals, which were washed with ice-cold methanol (2 mL) and thoroughly dried. Yield 69 mg (73%). IR (KBr): $\tilde{\nu}$ = (inter alia) 3294 (m), 3099 (m), 3061 (m), 3007 (m), 1635 (w), 1607 (m), 1592 (m), 1571 (w), 1521 (w), 1496 (m), 1456 (s), 1429 (m), 1295 (m), 1260 (m), 1057 (br. vs), 794 (m), 750 (m), 700 (m), 640 (w), 608 (w), 521 (w) cm^{-1} . Solution Vis/NIR (MeCN): λ_{max} ($\epsilon/\text{L mol}^{-1}\text{cm}^{-1}$) = 8700 (54), 11600 (37) cm^{-1} . Solid state vis/NIR (BaSO₄): λ_{max} (relative peak height) = 18900 (1), 11400 (0.67). ESI-MS (pos.): m/z = 859 $[\text{Ni}(\text{adpt})_3(\text{BF}_4)]^+$, 621 $[\text{Ni}(\text{adpt})_2(\text{BF}_4)]^+$, 386 $[\text{Ni}(\text{adpt})_3]^{2+}$, 267 $[\text{Ni}(\text{adpt})_2]^{2+}\cdot\text{1BF}_4$. $\text{C}_{36}\text{H}_{30}\text{B}_2\text{F}_8\text{N}_{18}\text{Ni}$ (947.05): calcd. C 45.66, H 3.19, N 26.62; found C 45.66, H 3.25, N 26.37.

[Ni(pldpt)₃(ClO₄)₂(2ClO₄): The reaction of $[\text{Ni}(\text{H}_2\text{O})_6](\text{ClO}_4)_2$ (18 mg, 0.05 mmol) and **pldpt** (43 mg, 0.15 mmol) in 6 mL of MeCN according to the procedure described above gave pale pink-purple microcrystals. Yield 41 mg (73%). IR (KBr): $\tilde{\nu}$ = (inter alia) 3170 (m), 2975 (m), 1610 (m), 1588 (w), 1505 (m), 1450 (s), 1430 (m), 1337 (m), 1297 (m), 1268 (w), 1089 (br. vs), 1016 (m), 992 (m), 912 (w), 793 (m), 738 (m), 705 (m), 642 (m), 623 (m) cm^{-1} . ESI-MS (pos.): m/z = 461 $[\text{Ni}(\text{pldpt})_3]^{2+}$, 289 $[\text{H}(\text{pldpt})]^+\cdot\text{2ClO}_4$. $\text{C}_{48}\text{H}_{36}\text{Cl}_2\text{N}_{18}\text{NiO}_8$ (1122.51): calcd. C 51.36, H 3.23, N 22.46; found C 51.07, H 3.54, N 22.24.

[Ni(pldpt)₃(BF₄)₂·2H₂O(2BF₄·2H₂O): The reaction of $[\text{Ni}(\text{H}_2\text{O})_6](\text{BF}_4)_2$ (34 mg, 0.10 mmol) and **pldpt** (87 mg, 0.30 mmol) in 12 mL of MeCN according to the procedure described above gave pale pink-purple microcrystals, which were washed with ice-cold methanol (2 mL) and thoroughly dried. Yield 70 mg (62%). IR (KBr): $\tilde{\nu}$ = (inter alia) 3141 (m), 3106 (m), 1611 (m), 1587 (w), 1572 (w), 1507 (w), 1479 (m), 1451 (s), 1432 (m), 1337 (m), 1297 (m), 1268 (w), 1057 (br. vs), 912 (w), 792 (m), 739 (m), 707 (m), 643 (m), 615 (m), 521 (w) cm^{-1} . Solution Vis/NIR (MeCN): λ_{max} ($\epsilon/\text{L mol}^{-1}\text{cm}^{-1}$) = 18800 (20), 11600 (16). Solid-state Vis/NIR (BaSO₄): λ_{max} (relative peak height) = 19100 (1), 11400 (0.68) cm^{-1} . ESI-MS (pos.): m/z = 599 $[\text{Na}(\text{pldpt})_2]^+$, 461 $[\text{Ni}(\text{pldpt})_3]^{2+}$, 311 $[\text{Na}(\text{pldpt})]^+\cdot\text{2BF}_4\cdot\text{2H}_2\text{O}$. $\text{C}_{48}\text{H}_{40}\text{B}_2\text{F}_8\text{N}_{18}\text{NiO}_2$ (1133.25): calcd. C 50.87, H 3.56, N 22.25; found C 51.09, H 3.52, N 22.35.

General Procedure for Synthesis of Complexes 1PF₆, 1SbF₆, 2PF₆ and 2SbF₆: One equivalent of anhydrous NiSO₄, two equivalents of sodium hexafluorophosphate or sodium hexafluoroantimonate, and three equivalents of the appropriate ligand were refluxed for one hour in MeCN, protected from atmospheric moisture with a calcium chloride drying tube. The resulting pink solution containing a fine white precipitate was cooled to room temperature, and then filtered to give a clear, pink solution. This was reduced in volume to ca. 8 mL and subjected to diethyl ether vapour diffusion, yielding pale purple-pink microcrystals, which were isolated by filtration, washed with diethyl ether, and dried thoroughly in vacuo. Yields ranged from 39 to 48%.

[Ni(adpt)₃(PF₆)₂·0.75H₂O (1PF₆·0.75H₂O): The reaction of NiSO₄ (12 mg, 0.08 mmol), NaPF₆ (27 mg, 0.16 mmol) and **adpt** (57 mg, 0.24 mmol) in 10 mL of MeCN according to the procedure de-

scribed above gave pale pink-purple microcrystals. Yield 37 mg (43%). IR (KBr): $\tilde{\nu}$ = (inter alia) 3313 (m), 3114 (m), 1608 (m), 1592 (m), 1497 (m), 1456 (m), 1430 (m), 1295 (w), 1259 (w), 1055 (w), 1017 (m), 843 (br. vs), 792 (m), 749 (m), 702 (m), 640 (w), 609 (w), 558 (s) cm^{-1} . ESI-MS (pos.): m/z = 1085 $[\text{Na}\cdot\text{Ni}(\text{adpt})_3(\text{PF}_6)_2]^+$, 267 $[\text{Ni}(\text{adpt})_2]^{2+}\cdot\text{1PF}_6\cdot\text{0.75H}_2\text{O}$. $\text{C}_{36}\text{H}_{31.5}\text{F}_{12}\text{N}_{18}\text{NiO}_{0.75}\text{P}_2$ (1076.87): calcd. C 40.17, H 2.95, N 23.42; found C 40.39, H 2.70, N 23.11.

[Ni(adpt)₃(SbF₆)₂ (1SbF₆): The reaction of NiSO₄ (12 mg, 0.08 mmol), NaSbF₆ (41 mg, 0.16 mmol) and **adpt** (57 mg, 0.24 mmol) in 15 mL of MeCN according to the procedure described above gave pale pink-purple microcrystals. Yield 39 mg (39%). IR (KBr): $\tilde{\nu}$ = (inter alia) 3309 (m), 1608 (m), 1592 (m), 1496 (m), 1455 (m), 1430 (m), 1293 (w), 1259 (w), 1016 (m), 795 (m), 750 (m), 703 (m), 661 (vs) cm^{-1} . ESI-MS (pos.): m/z = 1009 $[\text{Ni}(\text{adpt})_3(\text{SbF}_6)]^+$, 771 $[\text{Ni}(\text{adpt})_2(\text{SbF}_6)]^+$, 267 $[\text{Ni}(\text{adpt})_3]^{2+}\cdot\text{1SbF}_6$. $\text{C}_{36}\text{H}_{30}\text{F}_{12}\text{N}_{18}\text{NiSb}_2$ (1244.94): calcd. C 34.73, H 2.43, N 20.25; found C 34.84, H 2.41, N 20.22.

[Ni(pldpt)₃(PF₆)₂ (2PF₆·1.5H₂O): The reaction of NiSO₄ (12 mg, 0.08 mmol), NaPF₆ (27 mg, 0.16 mmol) and **pldpt** (69 mg, 0.24 mmol) in 20 mL of MeCN according to the procedure described above gave pale pink-purple microcrystals. Yield 43 mg (43%). IR (KBr): $\tilde{\nu}$ = (inter alia) 3153 (m), 3113 (m), 2872 (m), 1610 (m), 1588 (m), 1573 (w), 1505 (w), 1452 (s), 1430 (m), 1337 (m), 1298 (m), 1268 (w), 1155 (w), 1103 (w), 1017 (m), 913 (m), 843 (br. vs), 792 (m), 741 (m), 730 (m), 706 (m), 643 (m), 615 (w), 557 (s) cm^{-1} . ESI-MS (pos.): m/z = 1067 $[\text{Ni}(\text{pldpt})_3(\text{PF}_6)]^+$, 289 $[\text{H}(\text{pldpt})]^+\cdot\text{2PF}_6\cdot\text{1.5H}_2\text{O}$. $\text{C}_{48}\text{H}_{39}\text{F}_{12}\text{N}_{18}\text{NiO}_{1.5}\text{P}_2$ (1240.54): calcd. C 46.47, H 3.17, N 20.32; found C 46.68, H 3.47, N 20.38.

[Ni(pldpt)₃(SbF₆)₂·H₂O(2SbF₆·H₂O): The reaction of NiSO₄ (12 mg, 0.08 mmol), NaSbF₆ (41 mg, 0.16 mmol) and **pldpt** (69 mg, 0.24 mmol) in 15 mL of MeCN according to the procedure described above gave pale pink-purple microcrystals. Yield 54 mg (48%). IR (KBr): $\tilde{\nu}$ = (inter alia) 3145 (m), 1595 (m), 1572 (w), 1472 (s), 1430 (s), 1341 (m), 1292 (m), 1244 (w), 1156 (w), 1092 (m), 1076 (m), 1010 (m), 998 (w), 914 (m), 795 (s), 746 (s), 705 (m), 660 (vs) cm^{-1} . ESI-MS (pos.): m/z = 1157 $[\text{Ni}(\text{pldpt})_3(\text{SbF}_6)]^+$, 869 $[\text{Ni}(\text{pldpt})_2(\text{SbF}_6)]^+$, 461 $[\text{Ni}(\text{pldpt})_3]^{2+}$, 311 $[\text{Na}(\text{pldpt})]^+\cdot\text{2SbF}_6\cdot\text{H}_2\text{O}$. $\text{C}_{48}\text{H}_{38}\text{F}_{12}\text{N}_{18}\text{NiOSb}_2$ (1413.13): calcd. C 40.80, H 2.71, N 17.84; found C 40.84, H 2.74, N 17.80.

Supporting Information (see also the footnote on the first page of this article): Organic synthesis (Scheme S1) and reflectance and solution UV/Vis spectra for **2BF₄·2H₂O** and **1BF₄** (Figure S1) are given. Crystallographic information including complex geometries and packing interaction data (Tables S1–S9) as well as perspective views of complexes (Figures S2–S6) are also provided. Anion $\cdots\pi$ interaction analyses are presented (Figures S7–S12) as are color versions of Figures 2, 3 and 6.

Acknowledgments

This work was supported by the University of Otago, including a University of Otago Research Grant (to N. G. W. and S. B.). We thank the Tertiary Education Commission (New Zealand) for the award of a Bright Futures Top Achiever Doctoral scholarship to J. A. K. and the MacDiarmid Institute for Advanced Materials and Nanotechnology (to S. B.). We are grateful to Associate Professor Lyall Hanton (University of Otago) for helpful discussions and advice, and to Professor Helen Nicholson (University of Otago) for her help with the statistical analyses.

- [1] D. Quiñonero, C. Garau, C. Rotger, A. Frontera, P. Ballester, A. Costa, P. M. Deya, *Angew. Chem. Int. Ed.* **2002**, *41*, 3389–3392; M. Mascal, A. Armstrong, M. D. Bartberger, *J. Am. Chem. Soc.* **2002**, *124*, 6274–6276; I. Alkorta, I. Rozas, J. Elguero, *J. Am. Chem. Soc.* **2002**, *124*, 8593–8598; I. Alkorta, I. Rozas, J. Elguero, *J. Org. Chem.* **1997**, *62*, 4687–4691.
- [2] B. L. Schottel, H. T. Chifotides, K. R. Dunbar, *Chem. Soc. Rev.* **2008**, *37*, 68–83.
- [3] P. Gamez, T. J. Mooibroek, S. J. Teat, J. Reedijk, *Acc. Chem. Res.* **2007**, *40*, 435–444.
- [4] C. Garau, D. Quiñonero, A. Frontera, P. Ballester, A. Costa, P. M. Deya, *New J. Chem.* **2003**, *27*, 211–214.
- [5] P. de Hoog, P. Gamez, I. Mutikainen, U. Turpeinen, J. Reedijk, *Angew. Chem. Int. Ed.* **2004**, *43*, 5815–5817.
- [6] S. Demeshko, S. Dechert, F. Meyer, *J. Am. Chem. Soc.* **2004**, *126*, 4508–4509.
- [7] F. H. Allen, *Acta Crystallogr., Sect. B* **2002**, *58*, 380–388.
- [8] T. J. Mooibroek, C. A. Black, P. Gamez, J. Reedijk, *Cryst. Growth Des.* **2008**, *8*, 1082–1093.
- [9] C. S. Campos-Fernández, B. L. Schottel, H. T. Chifotides, J. K. Bera, J. Bacsá, J. M. Koomen, D. H. Russell, K. R. Dunbar, *J. Am. Chem. Soc.* **2005**, *127*, 12909–12923.
- [10] C. A. Black, L. R. Hanton, M. D. Spicer, *Chem. Commun.* **2007**, 3171–3173; I. y. A. Gural'skiy, P. V. Solntsev, H. Krautscheid, K. V. Domasevitch, *Chem. Commun.* **2006**, *46*, 4808–4810.
- [11] A. Frontera, F. Sączewski, M. Gdaniec, E. Dziemidowicz-Borys, A. Kurland, P. M. Deya, D. Quiñonero, C. Garau, *Chem. Eur. J.* **2005**, *11*, 6560–6567; M. Mascal, I. Yakovlev, E. B. Nikitin, J. C. Fettingner, *Angew. Chem. Int. Ed.* **2007**, *46*, 8782–8784; Y. S. Rosokha, S. V. Lindeman, S. V. Rosokha, J. K. Kochi, *Angew. Chem. Int. Ed.* **2004**, *43*, 4650–4652.
- [12] V. Gorteau, G. Bollot, J. Mareda, A. Perez-Velasco, S. Matile, *J. Am. Chem. Soc.* **2006**, *128*, 14788–14789; V. Gorteau, G. Bollot, J. Mareda, S. Matile, *Org. Biomol. Chem.* **2007**, *5*, 3000–3012.
- [13] P. D. Beer, P. A. Gale, *Angew. Chem. Int. Ed.* **2001**, *40*, 486–516.
- [14] P. Gütllich, Y. Garcia, H. A. Goodwin, *Chem. Soc. Rev.* **2000**, *29*, 419–427; O. Sato, J. Tao, Y.-Z. Zhang, *Angew. Chem. Int. Ed.* **2007**, *46*, 2152–2187.
- [15] J. A. Real, A. B. Gaspar, V. Niel, M. C. Muñoz, *Coord. Chem. Rev.* **2003**, *236*, 121–141.
- [16] J.-F. Létard, P. Guionneau, L. Goux-Capes, *Top. Curr. Chem.* **2004**, *234*, 221–250.
- [17] C. Rajadurai, O. Fuhr, R. Kruk, M. Ghafari, H. Hahn, M. Ruben, *Chem. Commun.* **2007**, 2636–2638; S. Cobo, G. Molnar, J. A. Real, A. Bousseksou, *Angew. Chem. Int. Ed.* **2006**, *45*, 5786–5789; V. Niel, A. Galet, A. B. Gaspar, M. C. Muñoz, J. A. Real, *Chem. Commun.* **2003**, 1248–1249; O. Kahn, C. J. Martinez, *Science* **1998**, *279*, 44–48.
- [18] Y. Sunatsuki, Y. Ikuta, N. Matsumoto, H. Ohta, M. Kojima, S. Iijima, S. Hayami, Y. Maeda, S. Kaizaki, F. Dahan, J.-P. Tuchagues, *Angew. Chem. Int. Ed.* **2003**, *42*, 1614–1618; G. S. Matouzenko, G. Molnar, N. Bréfuel, M. Perrin, A. Bousseksou, S. A. Borshch, *Chem. Mater.* **2003**, *15*, 550–556; M. Yamada, M. Ooidemizu, Y. Ikuta, S. Osa, N. Matsumoto, S. Iijima, M. Kojima, F. Dahan, J.-P. Tuchagues, *Inorg. Chem.* **2003**, *42*, 8406–8416; Y. Ikuta, M. Ooidemizu, Y. Yamahata, M. Yamada, S. Osa, N. Matsumoto, S. Iijima, Y. Sunatsuki, M. Kojima, F. Dahan, J.-P. Tuchagues, *Inorg. Chem.* **2003**, *42*, 7001–7017.
- [19] J.-F. Létard, P. Guionneau, E. Codjovi, O. Lavastre, G. Bravic, D. Chasseau, O. Kahn, *J. Am. Chem. Soc.* **1997**, *119*, 10861–10862; Z. J. Zhong, J.-Q. Tao, Z. Yu, C.-Y. Dun, Y.-J. Liu, X.-Z. You, *J. Chem. Soc., Dalton Trans.* **1998**, 327–328; R. Boča, M. Boča, L. Dlhán, K. Falk, H. Fuess, W. Haase, R. Jaroščiak, B. Papánková, F. Renz, M. Vrbová, R. Werner, *Inorg. Chem.* **2001**, *40*, 3025–3033.
- [20] Anion ordering/disordering involving a perchlorate anion that interacts with tetrazole ring has recently been implicated in a hysteretic SCO: M. Quesada, H. Kooijman, P. Gamez, J. S. Costa, P. J. v. Koningsbruggen, P. Weinberger, M. Reissner, A. L. Spek, J. G. Haasnoot, J. Reedijk, *Dalton Trans.* **2007**, 5434–5440.
- [21] J. F. Geldard, F. Lions, *J. Org. Chem.* **1965**, *30*, 318–319.
- [22] S. K. Mandal, H. J. Clase, J. N. Bridson, S. Ray, *Inorg. Chim. Acta* **1993**, *209*, 1–4.
- [23] a) M. H. Klingele, P. D. W. Boyd, B. Moubaraki, K. S. Murray, S. Brooker, *Eur. J. Inorg. Chem.* **2006**, 573–589; b) J. A. Kitchen, A. Noble, C. D. Brandt, B. Moubaraki, K. S. Murray, S. Brooker, *Inorg. Chem.* **2008**, *47*, 9450–9458.
- [24] K. H. Sugiyarto, D. C. Craig, A. D. Rae, H. A. Goodwin, *Aust. J. Chem.* **1995**, *48*, 35–54; K. H. Sugiyarto, H. A. Goodwin, *Aust. J. Chem.* **1988**, *41*, 1645–1663.
- [25] K. H. Sugiyarto, H. A. Goodwin, *Aust. J. Chem.* **1987**, *40*, 775–783.
- [26] M. H. Klingele, S. Brooker, *Eur. J. Org. Chem.* **2004**, 3422–3434.
- [27] C. Hansch, A. Leo, R. W. Taft, *Chem. Rev.* **1991**, *91*, 165–195.
- [28] M. P. Mingos, A. L. Rohl, *Inorg. Chem.* **1991**, *30*, 3769–3771.
- [29] G. S. Matouzenko, A. Bousseksou, S. Borshch, M. Perrin, S. Zein, L. Salmon, G. Molnar, S. Lecocq, *Inorg. Chem.* **2004**, *43*, 227–236.
- [30] M. Shaker, S. Parveen, N. Begum, Y. Azim, *Polyhedron* **2003**, *22*, 3181–3186.
- [31] J. A. Kitchen, N. G. White, B. Moubaraki, K. S. Murray, P. D. W. Boyd, M. Boyd, S. Brooker, manuscript in preparation.
- [32] B. L. Schottel, H. T. Chifotides, M. Shatruk, A. Chouai, L. M. Pérez, J. Bacsá, K. R. Dunbar, *J. Am. Chem. Soc.* **2006**, *128*, 5895–5902.
- [33] B. L. Schottel, J. Bacsá, K. R. Dunbar, *Chem. Commun.* **2005**, 46–47; C. S. Campos-Fernández, R. Clérac, J. M. Koomen, D. H. Russell, K. R. Dunbar, *J. Am. Chem. Soc.* **2001**, *123*, 773–774; C. S. Campos-Fernandez, R. Clerac, K. R. Dunbar, *Angew. Chem. Int. Ed.* **1999**, *38*, 3477–3479.
- [34] N. S. Oxtoby, A. J. Blake, N. R. Champness, C. Wilson, *Proc. Natl. Acad. Sci. USA* **2002**, *99*, 4905–4910.
- [35] T. J. Mooibroek, S. J. Teat, C. Massera, P. Gamez, J. Reedijk, *Cryst. Growth Des.* **2006**, *6*, 1569–1574.
- [36] Z. Lu, J. S. Costa, O. Roubeau, I. Mutikainen, U. Turpeinen, S. J. Teat, P. Gamez, J. Reedijk, *Dalton Trans.* **2008**, 3567–3573.
- [37] G. M. Sheldrick, Univ. of Göttingen, Germany, **1996**; R. H. Blessing, *Acta Crystallogr., Sect. A* **1995**, *51*, 33–38.
- [38] G. M. Sheldrick, *Acta Crystallogr., Sect. A* **2008**, *64*, 112–122.

Received: December 29, 2008

Published Online: February 26, 2009